IJCRT.ORG ISSN : 2320-2882

INTERNATIONAL JOURNAL OF CREATIVE RESEARCH THOUGHTS (IJCRT)

An International Open Access, Peer-reviewed, Refereed Journal

HYDROTHERMAL SYNTHESIS OF NANO-TIO_2 PHOTOCATALYST AND ITS CHARACTERIZATION

[1]Vidya Francis, [2]Ayswarya E P, [3]Ajalesh B Nair, [4]Eby Thomas Thachil
[1]Assistant Professor, [2]Assistant Professor, [3]Assistant Professor, [4]Professor
[1]Department of Chemistry, Carmel College, Mala, Thrissur, Kerala

Abstract: Nanoanatase having photocatalytic activity was successfully prepared by hydrothermal method under controlled conditions using Titanium-iso-propoxide. It is one of the most commonly used semiconductor oxide for environmental photocatalysis, being of low toxicity, insoluble in water and stable to photo and chemical corrosion over a wide range of pH. Their properties, which are determined by the preparation method, are very crucial in photocatalysis. The advantages of the hydrothermal method are that it is an easy method to obtain nanotube morphology, variation in the synthesis method can be implemented to enhance the properties of TiO_2 nanotubes, and it is a feasible method for different applications. A systematic characterization was done using XRD, BET, FTIR and SEM techniques. When compared to commercial form, nanostructures have several advantages like large surface area, controlled morphology, size, porosity to obtain desired surface chemistry.

Index Terms: TiO_2, Hydrothermal, anatase, photocatalyst

1.INTRODUCTION

Studies on the photochemical activity of pigments in commercial polyolefins have been mainly concerned with white pigments. Titanium dioxide (TiO_2) is the most widely studied of these, since it is technically outstanding in many respects (King, 1968). Anatase, brookite and rutile are the three crystalline forms of titania. Among these crytalline forms anatase-TiO_2 deserves more attention by virtue of its use as pigment (J.G. Balfour, 1994) and gas sensors (Y.C. Yeh et al,1989), catalysts (C.G. Bond et al, 1991; P.S.Awati et al, 2003) and photocatalysts (Hagfeldt et al, 1995; Y.H. Hsien et al, 2001; C. Lizama et al, 2002) in applications related to pollution control and in photovoltaics (N. Serpane et al, 2000). The catalytic and other properties of these materials strongly depend on the crystallinity, surface morphology, the particle sizes and preparation methods. TiO_2 nanoparticles have real advantages in relation to photocatalytic activity. Different preparation processes for them have been reported, such as sol–gel process (G. Colon et al, 2002), hydrolysis of inorganic salts (Y. Zhang et al, 2001), ultrasonic technique and hydrothermal process (X.M. Wu et al, 2001; E. Vigil et al, 2001; H. Zhang et al, 2001; X. Ju et al, 2002).

This study describes a rapid hydrothermal synthesis method to produce phase pure, monodisperse anatase particles with small grain size and high specific surface area at low temperature. Hydrothermal processing of either amorphous titania or a titanium containing precursor has been shown to be an ideal method for producing ultrafine (grain size< 10nm) anatase crystallites with high specific surface areas and high crystallinity, a property that is essential for photocatalytic reactions (J. Ovenstone et al, 2001).

II. MATERIALS AND METHODS

Materials

Titanium-iso-propoxide, $[Ti(OPr^i)_4]$ purchased from Alpha was used as titanium source for TiO_2 photocatalyst preparation. $Ti(OPr^i)_4$ was used without further purification. Glacial acetic acid ($C_2H_4O_2$, 99.5%) was used as a solvent. Distilled water was used for the hydrolysis of $Ti(OPr^i)_4$.

Preparation of nano-TiO_2 photocatalyst by hydrothermal method

The most popular technique to hydrolytically prepare nanocrystalline titania is hydrothermal processing, i.e., crystallization at elevated temperature and pressure in the presence of water (A.Rabenau et al, 1985). Hydrothermal crystallization is carried out in a sealed autoclave. A heating mantle or oven is used to raise the temperature above the standard boiling point of the solvent, at which point the evaporating solvent begins to generate a pressure inside the sealed vessel exclusively due to the refluxing solvent. Hydrothermal reaction times are often as short as 2 h and are rarely longer than 1-2 days. The following procedure was employed in this case.

10ml $Ti(OPr^i)_4$ was dissolved in 20ml acetic acid by stirring. After stirring for 10 minutes, 200ml distilled water was added dropwise from a burette at a rate of 1ml/min. The stirring without heating was continued till a clear solution was obtained. The clear solution was then transferred into a Teflon-lined autoclave. The autoclave was then maintained at 110^0C overnight without shaking or stirring. After the autoclave naturally cooled to room temperature, the sample soution (Fig.1) was transferred into a beaker and subjected to solvent evaporation at 110^0C for 2h. It was then dried in oven at 110^0C for a few minutes in a current of air. The sample was then calcined at 400^0C in the muffle furnace for different time intervals to ensure a crystalline product (Fig.2). During this processing titanium (IV) alkoxide reacts with water and forms Ti-O-Ti bridges to create solid TiO_2, according to the reaction;

$$Ti(OR)_4 + 2\,H_2O \rightarrow TiO_2 + 4\,ROH$$

Fig. 1 The solution obtained after hydrothermal treatment in an autoclave

Fig. 2 TiO_2 nano particles obtained after calcinations at 400^0C

Characterization of nanotitania

X-Ray diffraction

The crystalline phase of the hydrothermally synthesized TiO_2 nanoparticles was analyzed by X-ray powder diffraction (XRD) pattern obtained from Bruker D8 Advance Model Diffractometer with Cu Kα radiation in the region $2\theta = 10–80^0$ and Ni filter operating at 30kV and 20mA. The crystallite size of the anatase particles was calculated from the X-ray diffraction peak using Scherrer's equation (B. D. Cullity, 1978; L. E. Alexander, 1968);

$$d_{hkl} = k\lambda / (\beta \cos(2\theta))$$

where d_{hkl} is the average crystallite size (nm), λ is the wavelength of the Cu Kα radiation applied ($\lambda = 1.54A^0$), θ the Bragg's angle of diffraction, β the full-width at half maximum intensity of the peak observed at $2\theta = 25.3^0$ (converted to radians) (L.Q. Jing et al, 2001) and k the constant usually taken as 0.94.

Bulk density

The bulk density of the material was determined as per ASTM D 1895-96. The small end of the funnel is closed with hand or a suitable flat strip and 115±5 cm^3 of samples are poured into the funnel. Open the bottom of the funnel quickly and allow the material to flow freely into the cup. If caking occurs in the funnel, the material may be loosened with a glass rod. After the material has passed through the funnel immediately scrape off the excess on the top of the cup with a straight edge without shaking the cup. Weigh the material nearest to 0.1g and determine bulk density.

BET studies

Surface area of the titanium dioxide nano particles as well as commercial titania were measured using BET method. Measurements were carried out under nitrogen atmosphere using ASAP 2000 model, surface area and porosity analyzer. Surface area was determined using the equation,

$$S_{BET} = 4.353\ V_m$$

where S_{BET} is the surface area in m^2/g and V_m is the molar volume of adsorbate gas (N_2) at STP.

Fourier transform infrared spectroscopy

FTIR spectra of the commercial and synthesized TiO_2 in powder form was recorded in the range 400 to 4000 cm^{-1}.

Scanning electron microscopy

The surface morphology of TiO_2 was examined using a scanning electron microscope. The synthesized and commercial TiO_2 samples were sputter-coated with a thin layer of gold and examined under scanning electron microscope.

III.RESULTS AND DISCUSSION

X-Ray diffraction

The XRD pattern is shown in Figs. 3 to 7. All the sharp peaks observed belong to anatase-TiO_2. Rutile and brookite phases were absent as their characteristic d-spacing values were not observed. Apparently, a complete anatase TiO_2 crystalline phase was obtained.

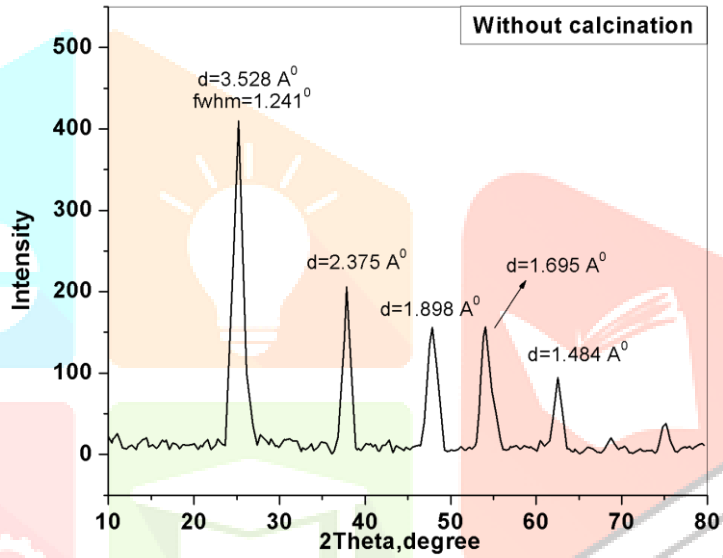

Fig.3 XRD pattern of hydrothermally synthesized nano-TiO_2 powder without calcination

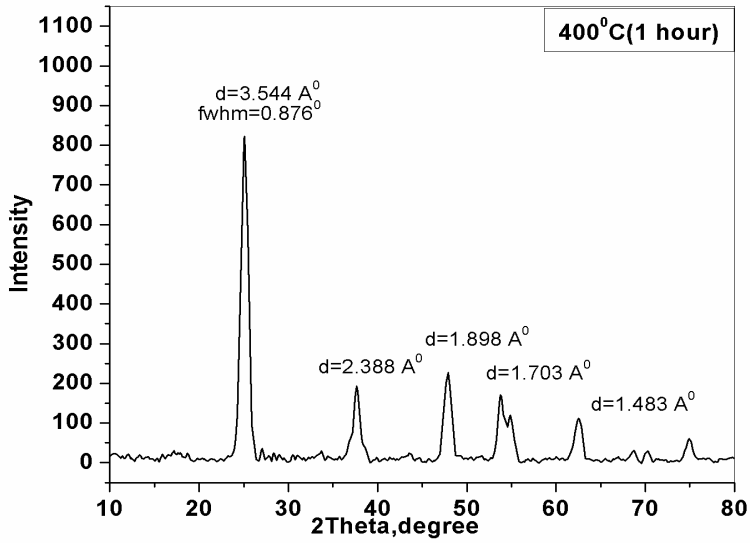

Fig.4 XRD pattern of hydrothermally synthesized nano-TiO_2 powder with calcination at 400^0C for 1 hour

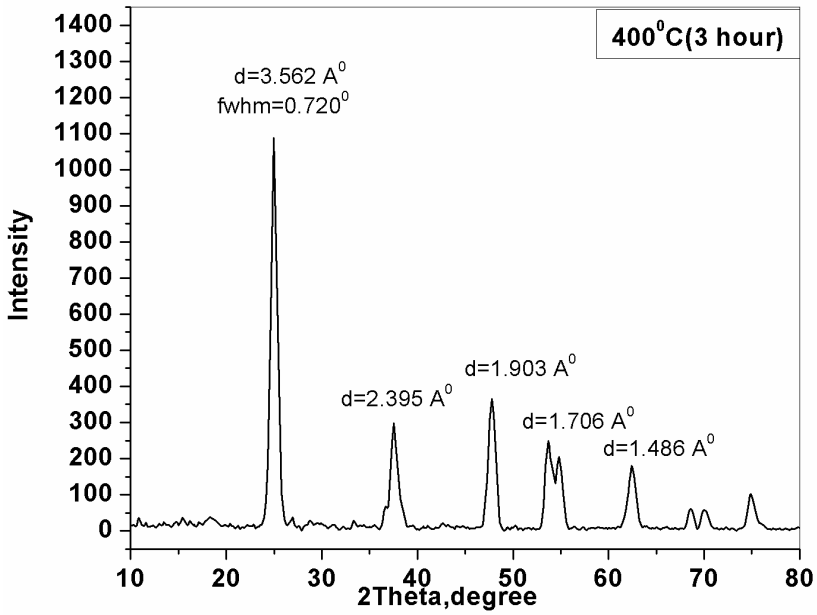

Fig.5 XRD pattern of hydrothermally synthesized nano-TiO_2 powder with calcination at 400^{0}C for 3 hours

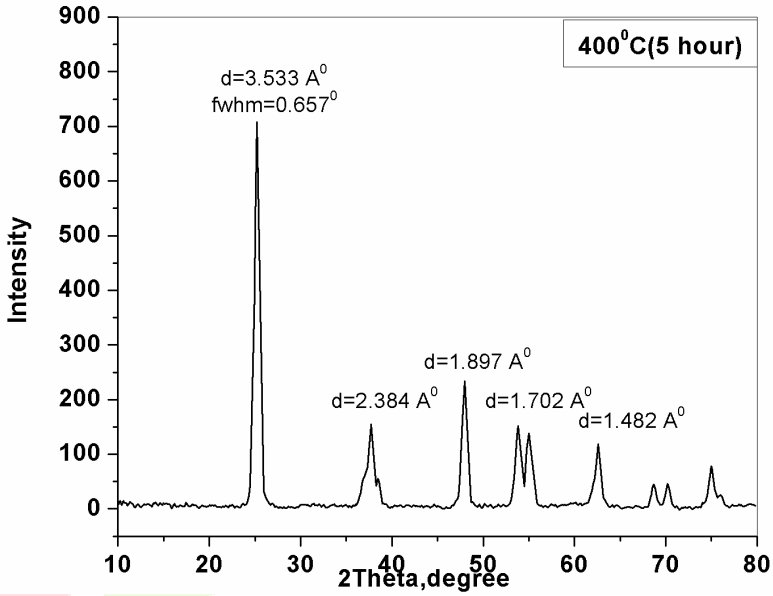

Fig.6 XRD pattern of hydrothermally synthesized nano-TiO_2 powder with calcination at 400^{0}C for 5 hours

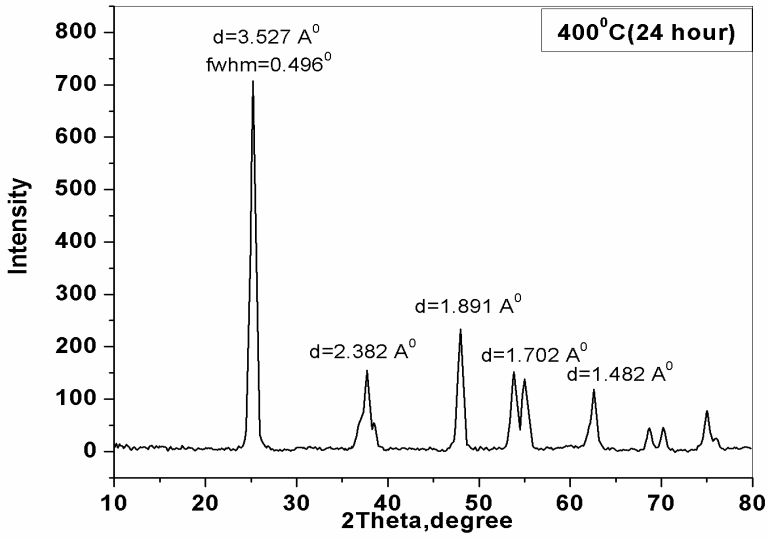

Fig.7 XRD pattern of hydrothermally synthesized nano-TiO_2 powder with calcination at 400^{0}C for 24 hours

Details of X-Ray diffraction studies are given in Table 1. Average crystallite size of TiO_2 was estimated by Scherrer's equation. The average crystallite size of the nano-TiO_2 (without calcinations) was estimated to be 6 nm and it is much lower than most other commercially available titania samples.

Table-1 Data of X-Ray diffraction studies

Catalyst	Calcination time (hour)	2θ (^{0})	Cos θ	β (^{0})	Crystallite size (nm)
A0	0	25.220	0.97	1.241	6.56
A1	1	25.108	0.97	0.876	9.29
A3	3	24.981	0.97	0.720	11.31
A5	5	25.188	0.97	0.657	12.39
A24	24	25.233	0.97	0.496	16.43

[A0 = Anatase sample without calcination, A1= Anatase sample after 1hour calcination, A3 = Anatase sample after 3hour calcination, A5 = Anatase sample after 5hour calcination, A24 = Anatase sample after 24hour calcination.]

The variation of β value and crystallite size with calcination time is shown in Figs. 8 and 9 respectively. The gradual narrowing of XRD lines with the increase in calcinations time (Fig. 8) reflects a corresponding increase in the average crystallite size (Fig. 9).

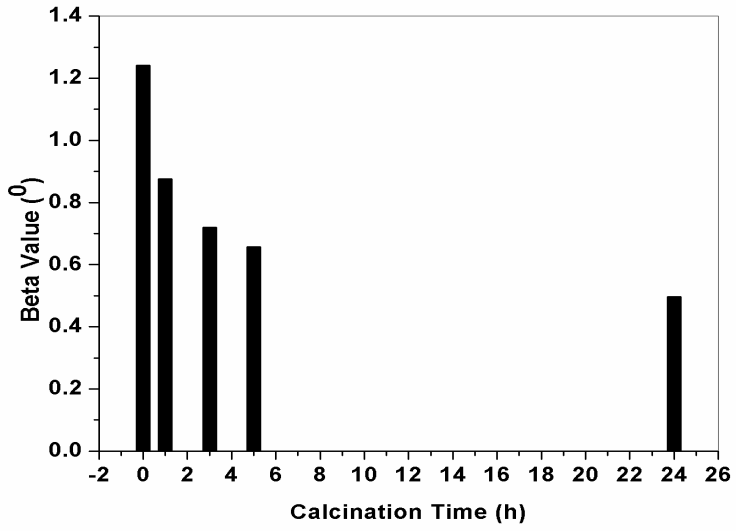

Fig. 8 Variation of β value with calcination time

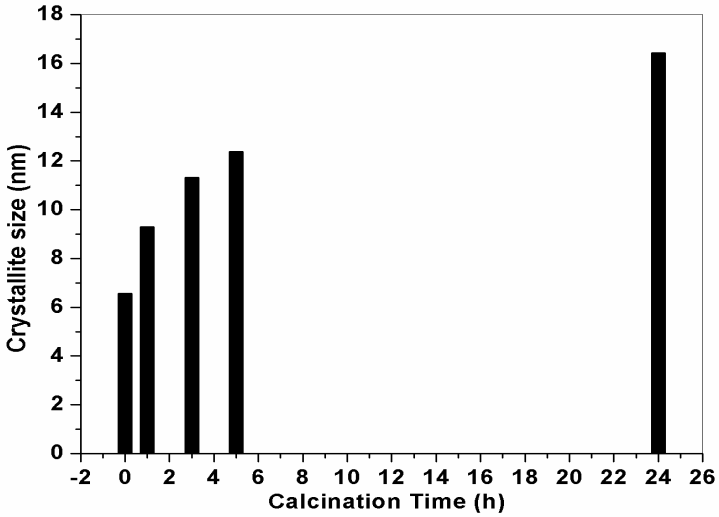

Fig. 9 Variation of crystallite size with calcination time

Bulk density

The bulk density of the commercial and synthesized samples is given in Table 2. It is found that the bulk density of the synthesized anatase (A0-A24) is higher than that of commercial anatase (A). This is due to the smaller particle size of synthesized anatase compared to that of commercial anatase.

Table-2 Bulk densities of the prepared anatase samples

Samples	Bulk density (g/cm^3)
A	0.979
A0	1.296
A1	1.282
A3	1.173
A5	1.136
A24	1.104

The variation of bulk density with calcination time is shown in Fig.10. Bulk density of the synthesized anatase samples decreases with increase in calcination time. This is due to the increase in particle size.

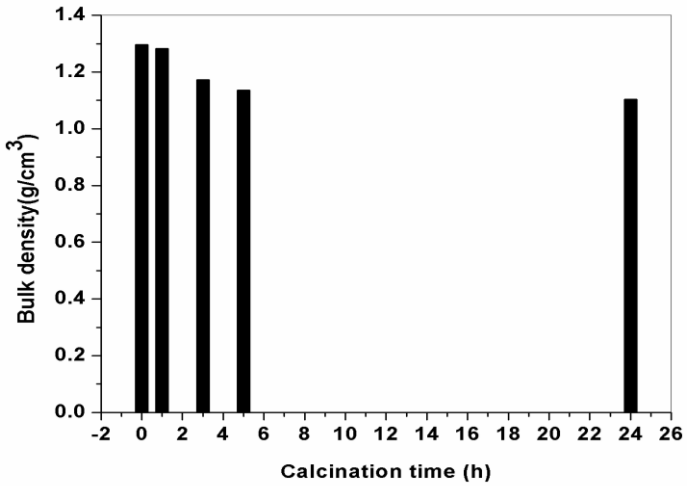

Fig.10. Variation of bulk density with calcination time

BET studies

Table 3 gives the BET adsorption results of nano and commercial anatase. From the table it is clear that nanoanatase has higher surface area than that of commercial anatase. Higher the surface area, lower the particle size. It is very well known that the photocatalytic effect of a catalyst is dependent on the crystallite size and surface area. The smaller the particles, the larger will be its specific surface area and the higher photocatalytic activity (M. Asilturk et al, 2005).

Table 3 Surface area of the TiO_2 samples

Samples	Surface area (m^2/g)
Commercial anatase	110
Nanoanatase	310

Infrared spectroscopy

The FTIR spectrum of nano and commercial forms of TiO_2 are shown in Figs. 11 and 12 respectivey. In the FTIR spectrum, the broad band at 3360 cm^{-1} is attributed to bound water. The peak at 1624 cm^{-1} is due to vibration frequency corresponding to the bending of water molecule (O-H bending vibration). Ti-(O-C) vibration is observed as a small band around 1053 cm^{-1}. The sharp band observed at 930 cm^{-1} is attributed to Ti-O stretching vibration.

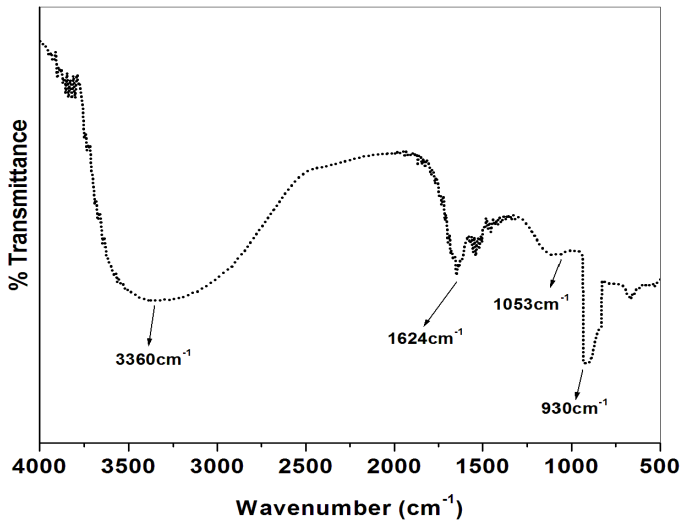

Fig. 11 FTIR spectrum of synthesized nano-TiO_2 particle dried at 110^{0}C

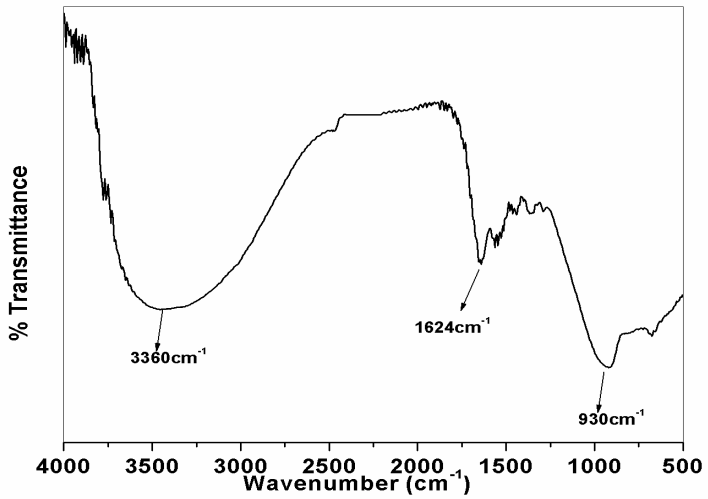

Fig. 12 FTIR spectrum of commercial-TiO_2

Scanning electron microscopy

The surface morphology of TiO_2 was examined by a JEOL JSM-6390LV Model scanning electron microscope. The scanning electron micrographs of the synthesized nano and commercial forms of TiO_2 are shown in Figs. 13 and 14. These micrographs show that the synthesized TiO_2 has lower particle size than the commercial TiO_2. From the micrographs it is clear that anatase particles are spherical in shape.

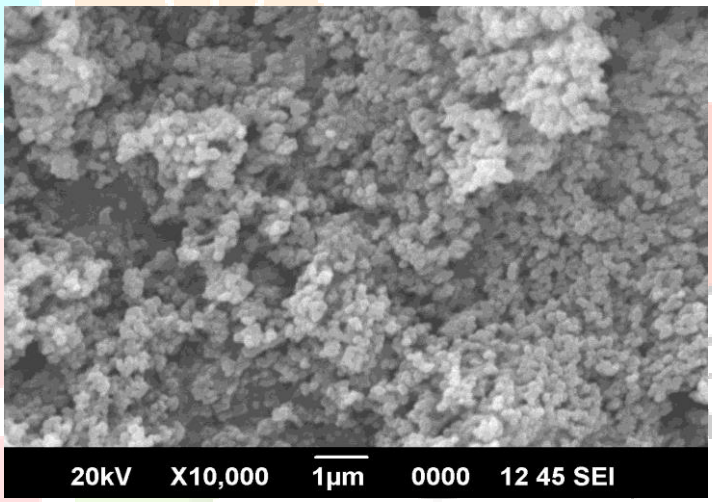

Fig.13 Typical SEM micrograph of hydrothermally synthesized nanoanatase particle

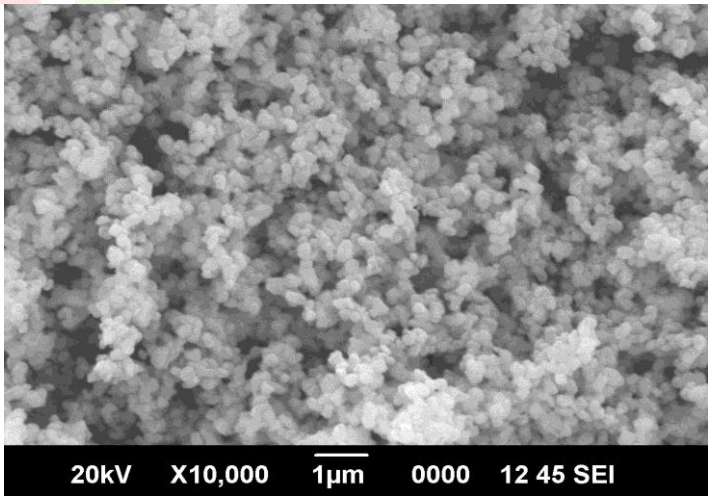

Fig. 14 Typical SEM micrograph of commercial anatase particle

IV.CONCLUSIONS

- Nanoanatase having photocatalytic activity was successfully prepared by hydrothermal method under controlled conditions.
- XRD studies showed that anatase was the only crystalline phase in the nano TiO_2 powder.
- The crystallite size of titania was calculated to be 6nm from the XRD results.
- Crystallite size increases as the calcination time of the synthesized anatase is increased.
- Anatase without any calcination showed the smallest crystallite size.
- From BET method the surface area was found to be $310m^2/g$ which is higher than that of commercial anatase ($110m^2/g$). Higher the surface area, lower the particle size.
- The smaller particle size and larger specific surface area indicates higher photocatalytic activity.
- SEM shows that nanoanatase prepared by this method is spherical in shape.

V. REFERENCES

[1] KING. 1968. Plastics and Polymers.
[2] J.G. Balfour. 1994. Technological Applications of Dispersions, Marcel Dekker, New York.
[3] Y.C. Yeh, T.T. Tseng, D.A. Chang. 1989. J. Am. Ceram. Soc.,72 ,1472.
[4] C.G. Bond, S. F. Tahir. 1991. Appl. Catal.,71, 1.
[5] P.S.Awati, S.V.Awate, P.P.Shah, V.Ramaswamy. 2003. Catal.Comm.,4, 393.
[6] Hagfeldt, M. Gratzel. 1995. Chem. Rev.,95,49.
[7] Y.H. Hsien, C.F. Chang, Y.H. Chen, S. Cheng. 2001. Appl. Catal., B Environ., 31, 241.
[8] C. Lizama, J. Freer, J. Baeza, H.D. Mansilla. 2002. Catal. Today, 76, 235.
[9] N. Serpane, J. Texier, A.V. Emeline, P. Pichat, H. Hidaka, J. Zhao; J. Photochem. Photobiol. 2000. A Chem.,136,145.
[10] G. Colon, M.C. Hidalgo, J.A. Navio. 2002. Catal. Today., 76, 91.
[11] Y. Zhang, G. Xion, N. Yao, W. Yang, X. Fu. 2001. Catal. Today., 68,220.
[12] X.M. Wu, L. Wang, Z.C. Tan, G.H. Li, S.S. Qu. 2001. J. Solid State Chem., 156, 220.
[13] E. Vigil, J.A. Ayllon, A.M. Peiro, R.R. Clemente. 2001. Langmuir,17,891.
[14] H. Zhang, M. Finnegan, J.F. Banfield. 2001. Nano Lett., 1, 81.
[15] X. Ju, P. Huang, N. Xu, J. Shi. 2002. J. Membr. Sci., 202, 63.
[16] J.Ovenstone. 2001. Journal of Materials Science., 36, 1325.
[17] A.Rabenau, C.Angewandte. 1985. International Edition English, 24, 1026.
[18] B. D. Cullity. 1978. Elements of X-Ray Diffraction, Addison Wesley.
[19] L. E. Alexander. 1968. X-ray diffraction methods in Polymer Science, John Wiley, New York.
[20] L.Q. Jing, Z. L. Xu, X. J. Sun, J. Shang, W. M. Cai. 2001. Appl. Surf. Sci. 180, 308.
[21] M. Asilturk, F. Sayilkan, S. Erdemoglu, M. Akarsu, H. Sayikan, M. Erdemoglu, E. Arpac. 2005 Journal of Hazardous Materials.